Scholte-wave excitation

Marine Denolle, Sjoerd de Ridder, Jason P. Chang, Eileen R. Martin, Taylor Dahlke, Humberto Arevalo-Lopez, Sr., and Stewart A. Levin[1]

ABSTRACT

We estimate the excitation of the Scholte waves using a new formulation of the surface-wave eigenproblem. We adapt the Rayleigh-wave case for solid media to accommodate the fluid shear-free condition and successfully calculate the Scholte-wave excitation. We detail here the derivation and numerical implementation, along with preliminary results for simple fluid-over-solid cases. We verify our results by comparing our phase velocity dispersion curve to the numerical solution of the dispersion relation for a fluid layer above an elastic half-space.

INTRODUCTION

A modal representation of interface waves can be used to construct waveform solutions to the wave equation. Free air-to-solid interface waves are commonly called Love and Rayleigh waves, solid-to-solid interface waves are usually called Stoneley waves, and fluid-to-solid interface waves, the focus of our interest, are referred to as Scholte waves. The excitation of these interface waves can be reduced to a generalized eigenproblem in the frequency domain. Denolle et al. (2012) solve this problem using a Chebyshev collocation method and successfully define the Rayleigh- and Love-wave modes for the single- and multi-layer solid cases. In this work, we generalize the code from Denolle et al. to handle a fluid layer at the surface in order to construct solutions for Scholte waves. We first expand on the implementation of boundary conditions at the fluid-to-solid interface in the generalized eigenproblem case. We then show the resulting eigenvalues and eigenfunctions for a simple two-layer, fluid-solid medium, which we validate against known algorithms.

INTRA-LIQUID FORMULATION

We first need to formulate the interface-wave eigenproblem with the proper boundary conditions to accommodate the fluid layer. Referring to the classic literature, e.g. Ewing et al. (1957), the behavior of waves in a fluid is correctly modeled by setting the shear modulus μ to zero in the equations for an isotropic elastic medium. In cylindrical coordinates, this makes equation 3 in Denolle et al. reduce to

---

[1] Chang, Dahlke and Martin are the main authors on the paper. Denolle and De Ridder led the summer mini seminar and authored the code and its modification respectively.

$$u = [r_1(k, z, \omega)\mathbf{S}_k^m(r, \phi) + ir_2(k, z, \omega)\mathbf{R}_k^m(r, \phi)]\, e^{-i\omega t} \ . \qquad \text{(3Den)}$$

In this formulation, $\mathbf{S}_k^m(r, \phi)$ is the gradient with respect to the radial and angular directions (holding depth constant) of $J_m(kr)e^{im\phi}$, and $J_m(\cdot)$ is a mth order Bessel function. $\mathbf{R}_k^m(r, \phi)$ is equal to $-J_m(kr)e^{im\phi}$. In other words, we project our solution on those vectors that describe modal solutions of the wave equation in cylindrical coordinates. The scalar stress-displacement values for the Rayleigh waves are (r_1, r_2, r_3, r_4), and (l_1, l_2) for the Love waves. For reference, explicit expressions for the Rayleigh wave r_3 and r_4 components are

$$r_3 = \sigma_{rz} = \mu \left(\frac{dr_1}{dz} - kr_2 \right) \quad \text{and}$$

$$r_4 = i\sigma_{zz} = k\lambda r_1 + (\lambda + 2\mu)\frac{dr_2}{dz} \ .$$

Equation 5 becomes

$$
\begin{aligned}
-\rho\omega^2 l_1 &= 0 \\
-\rho\omega^2 r_1 &= -k^2\lambda r_1 - k\lambda\frac{dr_2}{dz} \\
-\rho\omega^2 r_2 &= \frac{d}{dz}\left[\lambda\frac{dr_2}{dz} + k\lambda r_1\right]
\end{aligned}
\qquad , \qquad \text{(5Den)}
$$

and equation 9 reduces to

$$R_3 = k\lambda r_1 + \lambda\frac{dr_2}{dz} \ . \qquad \text{(9Den)}$$

Equation 8 yields

$$L_2 = [-i\sigma_{r\phi}] = 0 \ , \qquad \text{(8Den)}$$

and equation 10 becomes

$$R_4 = 0 \ . \qquad \text{(10Den)}$$

These last two equations are intuitive when coupled with $l_1 = 0$ from equation 5, as ideal liquids do not support shear waves. As a result, all nondiagonal stresses (particularly $\sigma_{r\phi}$ and σ_{rz}) are thus zero. The free-shear condition also presumes that the Love waves do not exist in the upper fluid layer. In other words, ignore the fluid when solving for Love wave modes.

For the Rayleigh eigenproblem, where ρ is the medium density, and λ and μ are the Lamé parameters, we can set μ and R_4 to zero from equation 12 to get

$$
\begin{bmatrix}
0 & -\frac{d}{dz} & \frac{1}{\lambda} & 0 \\
\frac{d}{dz} & 0 & 0 & -\frac{1}{0} \\
\rho\omega^2 & 0 & 0 & \frac{d}{dz} \\
0 & -\rho\omega^2 & -\frac{d}{dz} & 0
\end{bmatrix}
\begin{bmatrix}
r_1 \\ r_2 \\ R_3 \\ 0
\end{bmatrix}
= k
\begin{bmatrix}
r_1 \\ r_2 \\ R_3 \\ 0
\end{bmatrix} .
\tag{12Den}
$$

In order to have a system of three equations to solve for three unknowns, we eliminate a row of the matrix. Because of the singularity that arises in the second row of the matrix, we eliminate this equation, leaving the 3x3 system:

$$
\begin{bmatrix}
0 & -\frac{d}{dz} & \frac{1}{\lambda} \\
\rho\omega^2 & 0 & 0 \\
0 & -\rho\omega^2 & -\frac{d}{dz}
\end{bmatrix}
\begin{bmatrix}
r_1 \\ r_2 \\ R_3
\end{bmatrix}
= k
\begin{bmatrix}
1 & 0 & 0 \\
0 & 0 & 1 \\
0 & 0 & 0
\end{bmatrix}
\begin{bmatrix}
r_1 \\ r_2 \\ R_3
\end{bmatrix} .
\tag{12Den}
$$

FLUID-SOLID BOUNDARY CONDITIONS

For the Scholte waves, the fluid couples to the top of the elastic model with the continuity of vertical displacement and normal stress (Ewing et al., 1957; Aki and Richards, 1980). Following Denolle et al., this translates to the continuity of r_2 and $(\lambda + 2\mu)\frac{dr_2}{dz} + k\lambda r_1$, in addition to $R_4 = 0$. For the free surface, $\lambda \frac{dr_2}{dz} + \lambda k r_1 = 0$ is the appropriate free shear boundary condition.

At the fluid-solid interface, we want continuity of $(\lambda + 2\mu)\frac{dr_2}{dz} + \lambda k r_1$, and can use equation 9 from Denolle et al. to translate this to a condition on R_3:

$$
\begin{aligned}
(\lambda + 2\mu)\frac{dr_2}{dz} + \lambda k r_1 &= \frac{\lambda + 2\mu}{\lambda}\left(R_3 - k(\lambda + 2\mu)r_1\right) + \lambda k r_1 \\
&= \left(1 + \frac{2\mu}{\lambda}\right)R_3 + k\left(\lambda - \frac{(\lambda + 2\mu)^2}{\lambda}\right)r_1 .
\end{aligned}
$$

IMPLEMENTATION

We strove to keep the implementation as simple as possible. To this end, our code alters the boundary conditions for the surface and fluid-solid interface as described above and selects only a subset of the equations within the liquid layer.

For both the Love- and Rayleigh-wave eigenvalue problems, we can write the eigenvalue system generally as $A\mathbf{x} = kB\mathbf{x}$, where B is mostly an identity matrix except for a few entries altered for boundary conditions. We create the matrices A and B as though modeling solid layers for which μ just happens to equal zero in the top layer, as described in Denolle et al. (2012). Then we apply matrices to the left and right of these to select the relevant rows and columns so that we solve a new eigenvalue problem, $L_r A L_c \mathbf{x} = k L_r B L_c \mathbf{x}$.

For the Love waves, we remove both of the equations related to the water layer since we know the solution will be zero in a liquid. For example, consider a liquid layer above a solid layer with constant parameters within each layer. In this case, the matrices selecting rows and columns are

$$
L_r = L_c^* = \left[\begin{array}{cc|cc} I_{N_s} & 0_{N_s} & 0_{N_l} & 0_{N_l} \\ 0_{N_s} & I_{N_s} & 0_{N_l} & 0_{N_l} \end{array} \right] \; ,
$$

where N_s and N_l are the number of points in the solid and liquid layer, respectively, 0_n represents the zero matrix of size $n \times n$, and I_n represents the $n \times n$ identity matrix.

For the Rayleigh wave we have a set of four equations. In the liquid layer, we set the shear wave speed to zero. Equation 12Den shows that we select only the first, third and fourth rows and the first, second and third columns of the matrices' liquid section. Looking again at the example of a liquid layer above a single solid layer, we achieve this by choosing our row and column selection matrices as follows

$$
L_r = \left[\begin{array}{c|cccc} I_{4 \times N_s} & 0 & 0 & 0 & 0 \\ \hline 0 & I_{N_l} & 0 & 0 & 0 \\ 0 & 0 & 0 & I_{N_l} & 0 \\ 0 & 0 & 0 & 0 & I_{N_l} \end{array} \right] \; , \qquad
L_c = \left[\begin{array}{c|ccc} I_{4 \times N_s} & 0 & 0 & 0 \\ \hline 0 & I_{N_l} & 0 & 0 \\ 0 & 0 & I_{N_l} & 0 \\ 0 & 0 & 0 & I_{N_l} \\ 0 & 0 & 0 & 0 \end{array} \right] \; .
$$

RESULTS

We display results from the modified code for a fluid-solid interface. The model parameters that we used are shown in Figure 1. For our calculations, both layers contain 50 collocation points. We assume that the solid is a Poisson medium when computing our associated Lamé parameters.

Figure 1: Profile of our 1D model of a fluid layer over a solid. Left: P-wave (red) and S-wave (blue) velocities with depth. Right: Density with depth. [**CR**]
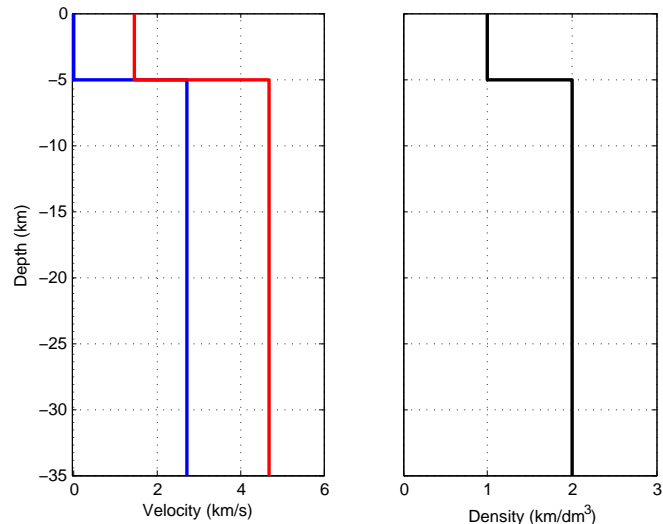
Figure 2 shows the computed fundamental-mode Scholte displacement eigenfunctions for the previously described 1D medium. We show the Scholte-wave eigenfunctions for three frequencies: 0.05, 0.10, and 1.00 Hz. We see that the horizontal displacement (r_1) is discontinuous at the fluid-solid interface and that the vertical displacement (r_2) is continuous, which are the boundary conditions that we imposed. We also see that the eigenfunction is more sensitive to the interface at higher frequencies than at lower frequencies. This makes sense, since lower frequencies have longer wavelengths that will be less affected by the interface. Figure 3, computed using the Haskell matrix codes of Herrmann (2010), further confirms the validity of our modifications.
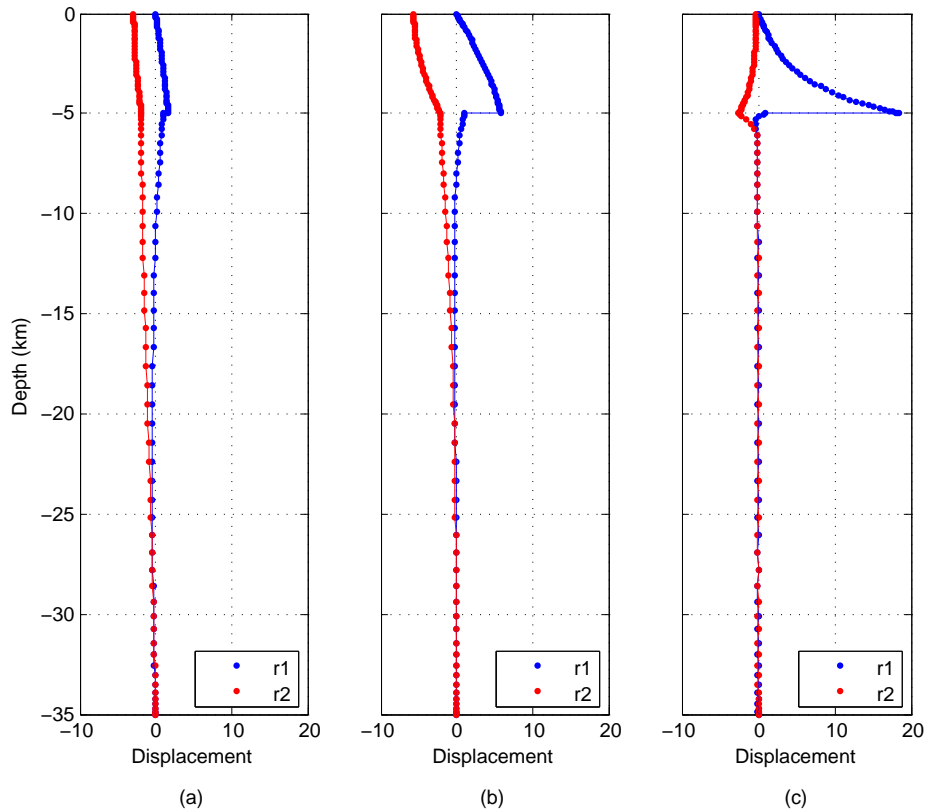

Figure 2: Displacement eigenfunctions for the described fluid-solid 1D medium. For Scholte waves: (a) 0.05 Hz, (b) 0.10 Hz, and (c) 1.00 Hz. r_1 is the horizontal displacement and r_2 is the vertical displacement. [**CR**]

Figure 4 shows the computed fundamental mode Scholte-wave stress eigenfunctions. Again, we show the eigenfunctions for three frequencies: 0.05, 0.10, and 1.00 Hz. We see that the shear stress (R_3) is discontinuous at the interface, and that the normal stress (R_4) is continuous across the interface. These observations are what we expect. Also note that much like with the displacement eigenfunctions, sensitivity of the stress eigenfunctions at the fluid-solid interface increases with frequency. Again, this is likely related to lower frequencies having longer wavelengths and hence being less sensitive to relatively shallow interfaces.

Figure 3: 1.00 Hz displacement eigenfunctions for the described fluid-solid 1D medium computed using the Haskell matrix method. Except for the packaged choices for overall normalization and the sign for radial motion, this is in good agreement with Figure 2. [**CR**]
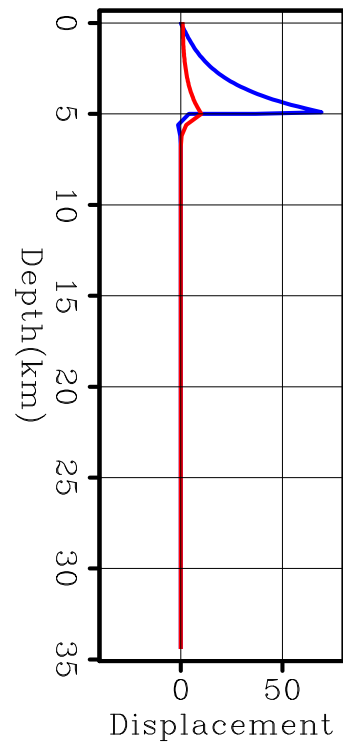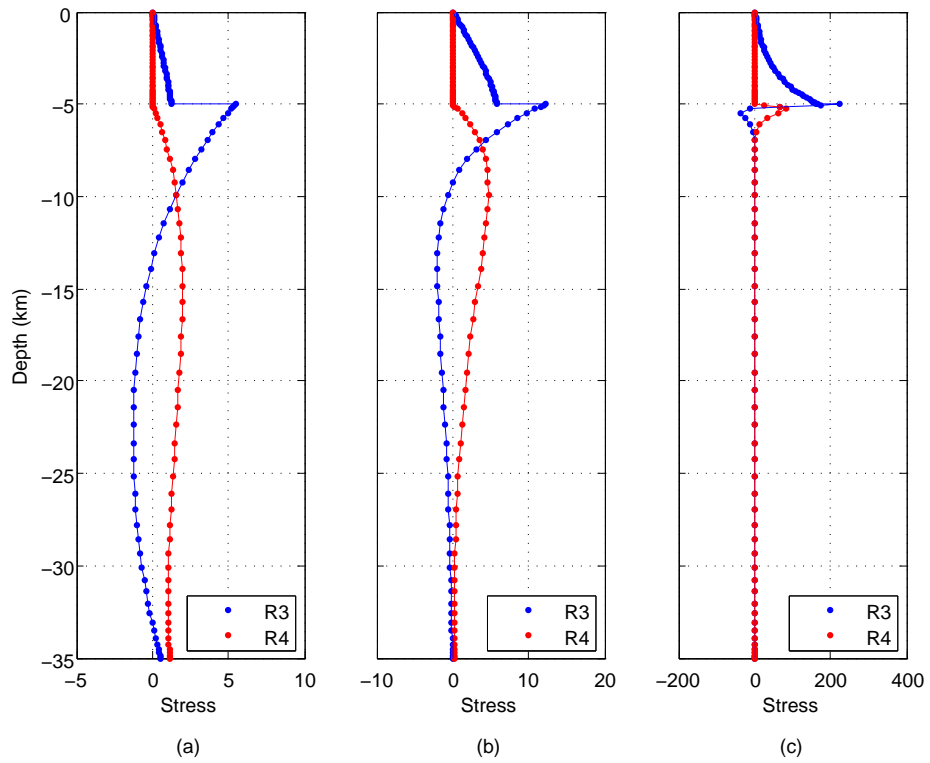
Figure 4: Scholte-wave stress eigenfunctions for the described fluid-solid 1D medium at (a) 0.05 Hz, (b) 0.10 Hz, and (c) 1.00 Hz. R3 is the shear stress and R4 is the normal stress. Note that the scales on stress differ between each frequency. [**CR**]

To view the eigenvalues (wavenumbers), we plot phase velocity dispersion curves for Scholte waves in Figure 5. We obtain these curves by solving

$$c_S = \frac{\omega}{k_S(\omega)}, \tag{1}$$

where c_S is the Scholte-wave phase velocity, ω is angular frequency, and k_S is wavenumber as a function of frequency. To verify these results, we compare these dispersion curves to the numerically calculated Scholte wave phase velocity, c, which is the solution to the dispersion relation for a finite fluid layer over an elastic half-space (Biot, 1952). The relation is given as

$$4\sqrt{1 - \frac{c}{v_s}^2} - \frac{(2 - \frac{c}{v_s}^2)^2}{\sqrt{1 - \frac{c}{v_p}^2}} = \frac{\rho_f}{\rho_s} \frac{\frac{c}{v_s}^4}{\sqrt{\frac{c}{v_f}^2 - 1}} \tan\left[kh\sqrt{\frac{c}{v_f}^2 - 1}\right] \text{ for } \frac{c}{v_f} > 1 , \tag{2}$$

$$4\sqrt{1 - \frac{c}{v_s}^2} - \frac{(2 - \frac{c}{v_s}^2)^2}{\sqrt{1 - \frac{c}{v_p}^2}} = \frac{\rho_f}{\rho_s} \frac{\frac{c}{v_s}^4}{\sqrt{1 - \frac{c}{v_f}^2}} \tanh\left[kh\sqrt{1 - \frac{c}{v_f}^2}\right] \text{ for } \frac{c}{v_f} < 1 , \tag{3}$$

where k is wavenumber, h is the depth of the fluid layer, ρ_f is the fluid density, and ρ_s is the solid density. Furthermore, $\eta_1 = \frac{c}{v_s}$, $\eta_2 = \frac{c}{v_p}$, $\eta_f = \frac{c}{v_f}$, v_p is P-wave velocity in the solid, v_s is the S-wave velocity in the solid, and v_f is the velocity in the fluid.
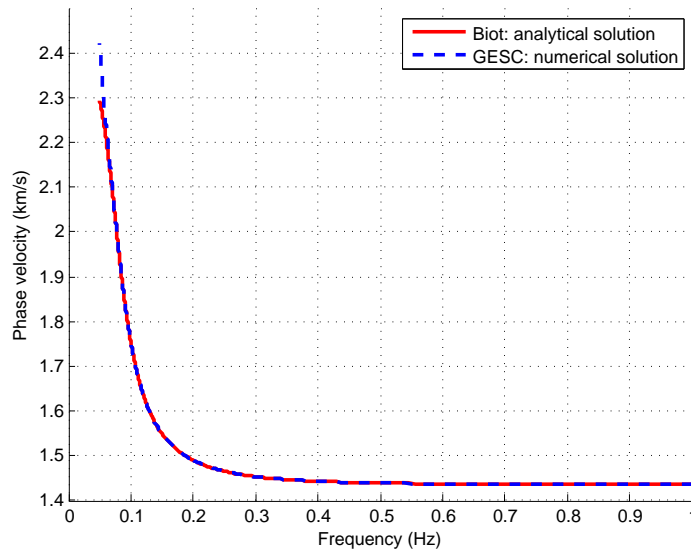

Figure 5: A comparison of phase velocity dispersion curves for a fluid-solid interface. Blue: our code. Red: numerical solution of the analytically-derived dispersion relation from Biot (1952). The solutions match up very well, suggesting that our modifications are correct. [**CR**]

Figure 5 shows that the numerically calculated reference solution (red) and our solution (blue) to the Scholte-wave dispersion relation match very well. The deviation between the two solutions at frequencies below 0.1 Hz reflects our approximation

of the half-space with a thick layer which has a rigid bottom boundary condition. Therefore, at these lower frequencies, we are approaching wavelengths that are longer than the domain of the model, causing our phase velocities to deviate from the numerical solution. Regardless, there is a clear match for the higher frequencies, which suggests that our calculated eigenfunctions and eigenvalues are indeed correct for Scholte waves.

CONCLUSIONS

Denolle et al. (2012) obtained the Rayleigh- and Love-wave solutions to the elastic wave equation by posing the problem in the generalized matrix eigenvalue framework. Here we expanded this framework to also solve for Scholte waves, and added this functionality to their code. We verified our theory and its implementation by finding that our phase velocity dispersion curves match well with the numerical solution to the dispersion relation for a finite liquid layer over an elastic half space of Biot (1952). We also found that our displacement eigenfunctions match well with those from the Haskell matrix codes of Herrmann (2010).

ACKNOWLEDGMENTS

REFERENCES

Aki, K. and P. G. Richards, 1980, Quantitative seismology, volume **1424**: Freeman San Francisco.

Biot, M. A., 1952, The interaction of Rayleigh and Stoneley waves in the ocean bottom: Bulletin of the Seismological Society of America, **42**, 81–93.

Denolle, M. A., E. M. Dunham, and G. C. Beroza, 2012, Solving the surface-wave eigenproblem with Chebyshev spectral collocation: Bulletin of the Seismological Society of America, **102**, 1214–1223.

Ewing, W. M., W. S. Jardetzky, F. Press, and A. Beiser, 1957, Elastic waves in layered media: Physics Today, **10**, 27.

Herrmann, R. B., 2010, Computer programs in seismology, version 3.33.